

Effects of Sulfur Substitution on Chemical Bonding Nature and Electrochemical Performance of Layered $\text{LiMn}_{0.9}\text{Cr}_{0.1}\text{O}_{2-x}\text{S}_x$

Seung Tae Lim,^{†,‡} Dae Hoon Park,[†] Sun Hee Lee,[†] Seong-Ju Hwang,^{†,*} Young Soo Yoon,^{†,‡} and Seong-Gu Kang[§]

[†]Center for Intelligent Nano-Bio Materials (CINBM), Division of Nano Sciences and Department of Chemistry Ewha Womans University, Seoul 120-750, Korea. *E-mail: hwangsju@ewha.ac.kr

[‡]Department of Advanced Technology Fusion, Konkuk University, Seoul 143-701, Korea. *E-mail: ysyoon@konkuk.ac.kr

[§]Department of Chemical Engineering, Hoseo University, Chungnam 336-795, Korea

Received July 22, 2006

Sulfur-substituted $\text{LiMn}_{0.9}\text{Cr}_{0.1}\text{O}_{2-x}\text{S}_x$ ($0 \leq x \leq 0.1$) layered oxides have been prepared by solid state reaction under inert atmosphere. From powder X-ray diffraction analyses, all the present lithium manganates were found to be crystallized with monoclinic-layered structure. Electrochemical measurements clearly demonstrated that, in comparison with the pristine $\text{LiMn}_{0.9}\text{Cr}_{0.1}\text{O}_2$, the sulfur-substituted derivatives exhibit smaller discharge capacities for the entire cycle range but the recovery of discharge capacity after the initial several cycles becomes faster upon sulfur substitution. The effect of the sulfur substitution on the chemical bonding nature of $\text{LiMn}_{0.9}\text{Cr}_{0.1}\text{O}_{2-x}\text{S}_x$ has been investigated using X-ray absorption spectroscopic (XAS) analyses at Mn and Cr K-edges. According to Mn K-edge XAS results, the trivalent oxidation state of manganese ion remains unchanged before and after the substitution whereas the local structure around manganese ions becomes more distorted with increasing the substitution rate of sulfur. On the other hand, the replacement of oxygen with sulfur has negligible influence on the local atomic arrangement around chromium ions, which is surely due to the high octahedral stabilization energy of Cr^{+III} ions. Based on the present experimental findings, we have suggested that the decrease of discharge capacity upon sulfur substitution is ascribable to the enhanced structural distortion of MnO_6 octahedra and/or to the formation of covalent Li-S bonds, and the accompanying improvement of cyclability would be related to the depression of Mn migration and/or to the pillaring effect of larger sulfur anion.

Key Words : Sulfur substitution, Layered lithium manganate, Structural distortion, Cyclability, Mn migration

Introduction

Over the past decades, lithium ion battery (LIB) has been established as one of the most important portable power sources for personal electronic devices, mobile telecommunication devices, electrical vehicles, and so on. Currently the layered LiCoO_2 compound is being applied for most of commercialized LIB cells due to its high energy density and its excellent stability with respect to extended electrochemical cyclings.¹ However, from the economic and environmental point of view, the high cost and high toxicity of cobalt have led to considerable research efforts to develop manganese-based materials as an alternative cathode.² Among various lithium manganese oxides ever synthesized, the layered LiMnO_2 compound exhibits a very large initial capacity of more than 270 mAh/g but it suffers from severe capacity fading which is surely ascribable to the irreversible transition to spinel-type structure.³⁻⁵ For the purpose of optimizing the electrochemical performance of this layered compound, numerous attempts have been made to enhance the structural stability of this layered phase with respect to repeated electrochemical cycles. As a consequence, it has been well-established that the partial substitution of manganese ions with other transition metal ions such as Cr^{+III} and Co^{+III} is quite effective in improving the cyclability of LiMn_2O_4 spinel.^{6,7} This phenomenon is attributable to the

fact that the incorporation of chromium or cobalt ions with large octahedral site stabilization energy (OSSE) hinders the migration of manganese ions into the interlayer lithium sites.⁶ However, such a cation substitution cannot prevent completely the structural modification during electrochemical cycling. Recently sulfur substitution has been known to be very useful in enhancing the electrochemical performance of spinel-structured LiMn_2O_4 electrode.^{8,9} In the light of this, it is highly feasible that the electrochemical performance of layered lithium manganese oxide can be optimized through the incorporation of sulfur. Very recently, it was reported that the sulfur-doped layered $\text{Li}_x\text{MnO}_{2-y}\text{S}_y$ synthesized by an ion-exchange method has better cyclability compared to the unsubstituted Li_xMnO_2 one.¹⁰ However, there have been no systematic studies on the effect of sulfur substitution on the chemical bonding nature and crystal structure of layered lithium manganese oxide. Moreover, the solid-state synthesis of sulfur-substituted layered lithium manganate has never been tried, although this method is much more favorable for mass-production than the previously reported ion-exchange method requiring the preparation and handling of air-sensitive sodium-containing precursor.¹⁰

In this work, we have prepared sulfur-substituted $\text{LiMn}_{0.9}\text{Cr}_{0.1}\text{O}_{2-x}\text{S}_x$ layered oxides through the solid-state reaction and characterized their electrochemical properties. Also, we have carried out X-ray diffraction (XRD) and X-ray absorp-

tion spectroscopic (XAS) analyses on these compounds to investigate the influence of sulfur substitution on their crystal structure and chemical bonding character.

Experimental Section

Layered $\text{LiMn}_{0.9}\text{Cr}_{0.1}\text{O}_{2-x}\text{S}_x$ ($0 \leq x \leq 0.1$) samples were prepared by conventional solid state reaction with the stoichiometric mixture of Li_2S , Li_2CO_3 , Mn_2O_3 , and Cr_2O_3 in the mole ratio of $2x : 1-2x : 0.9 : 0.1$. The heat-treatment was carried out at 960°C for 12 hr under N_2 flow. In order to minimize the evaporation of sulfur during heat-treatment, the mixture pellets were sintered in a covered alumina boat under the presence of excess sulfur element. The crystal structure of $\text{LiMn}_{0.9}\text{Cr}_{0.1}\text{O}_{2-x}\text{S}_x$ was studied by XRD measurement using Ni-filtered $\text{Cu K}\alpha$ radiation with a graphite diffracted beam monochromator, and their sulfur contents were determined using energy dispersive spectrometry (EDS). The electrochemical measurements were performed with the cell of $\text{Li}/1 \text{ M LiPF}_6$ in EC : DEC (50 : 50 v/v)/ $\text{LiMn}_{0.9}\text{Cr}_{0.1}\text{O}_{2-x}\text{S}_x$, which was assembled in a dry-box. The composite cathode was prepared by mixing thoroughly the active $\text{LiMn}_{0.9}\text{Cr}_{0.1}\text{O}_{2-x}\text{S}_x$ cathode material (85%) with 10% of acetylene black and 5% of PTFE (polytetrafluoroethylene). All the experiments were carried out in a galvanostatic mode with the constant current density of 6.25 or 20 mAh/g in the voltage range of 2.0–4.3 V.

XAS experiments were performed for $\text{LiMn}_{0.9}\text{Cr}_{0.1}\text{O}_{2-x}\text{S}_x$ ($x = 0, 0.05, \text{ and } 0.1$) by using the extended X-ray absorption fine structure (EXAFS) facility installed at the beam line 7C at the Pohang Accelerator Laboratory (PAL) in Pohang, Korea. The XAS data were collected at room temperature in a transmission mode using gas-ionization detectors. All the present spectra were calibrated by measuring the spectra of Mn and Cr metal foils. The data analysis for the experimental spectra was performed by the standard procedure as reported previously.¹¹ All the present X-ray absorption near-edge structure (XANES) spectra were normalized by fitting the smooth EXAFS high-energy region with a linear function after subtracting the background extrapolated from the pre-edge region.

Results and Discussion

Figure 1 represents the powder XRD patterns of sulfur-substituted $\text{LiMn}_{0.9}\text{Cr}_{0.1}\text{O}_{2-x}\text{S}_x$ ($x = 0, 0.05, \text{ and } 0.1$) layered oxides, together with that of spinel structured LiMn_2O_4 . All of the present $\text{LiMn}_{0.9}\text{Cr}_{0.1}\text{O}_{2-x}\text{S}_x$ compounds show nearly the same patterns with well-developed (hkl) reflections,

which can be well indexed on the basis of the monoclinic layered structure with the space group of $\text{C}2/m$.³ No trace of impurity phase is observable in the present patterns, indicating the formation of single-phase layered compounds in the sulfur substitution range applied here. From least square fitting analysis, lattice parameters and unit cell volumes of these layered compounds were calculated and summarized in Table 1. The replacement of oxide ions with sulfide ones gives rise to the expansion of unit cell volume, which is surely due to the larger radius of sulfide anion than oxide one ($\text{S}^{2-}(\text{VI}) = 1.70 \text{ \AA}$ and $\text{O}^{2-}(\text{VI}) = 1.26 \text{ \AA}$, the number in parenthesis denotes the coordination numbers of an ion).¹² The stabilization of sulfur ions in the lattice of layered lithium manganese oxide was cross-confirmed by EDS analysis and obtained sulfur contents are listed in Table 1.

We have performed Mn K- and Cr K-edge XANES analyses to investigate the variation of oxidation state and local symmetry of manganese and chromium ions upon sulfur substitution. The Mn K-edge XANES spectra for $\text{LiMn}_{0.9}\text{Cr}_{0.1}\text{O}_{2-x}\text{S}_x$ ($x = 0, 0.05, \text{ and } 0.10$) are shown in Figure 2, in comparison with reference spectra for Mn_2O_3 and MnO_2 . Despite notable differences in peak intensities, all the lithium manganese oxides exhibit common spectral features that are characteristic of the layered LiMnO_2 phase and indicative of similar chemical environment of manganese ion in the present compounds. In the pre-edge region, one or two small features denoted as P and P'

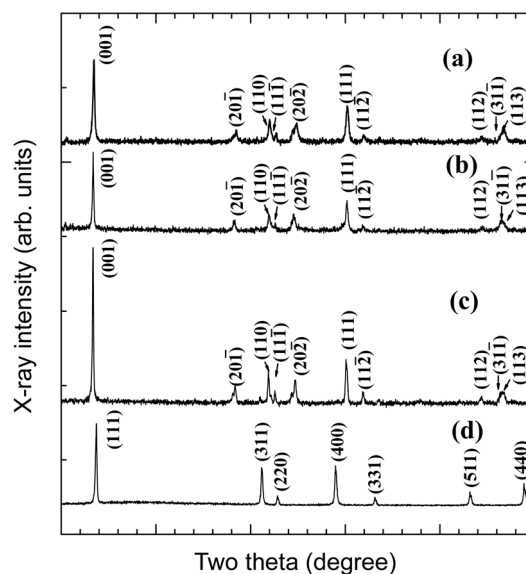


Figure 1. Powder XRD patterns for the layered $\text{LiMn}_{0.9}\text{Cr}_{0.1}\text{O}_{2-x}\text{S}_x$ compounds with $x =$ (a) 0, (b) 0.05, and (c) 0.1, in comparison with that for (d) cubic spinel LiMn_2O_4 .

Table 1. Lattice parameters, crystal symmetries, unit cell volumes, and sulfur contents of the layered $\text{LiMn}_{0.9}\text{Cr}_{0.1}\text{O}_{2-x}\text{S}_x$ compounds

Nominal composition	a (Å)	b (Å)	c (Å)	β (°)	V_c	S/Mn
$\text{LiMn}_{0.9}\text{Cr}_{0.1}\text{O}_2$	5.443	2.810	5.392	116.012	74.12	–
$\text{LiMn}_{0.9}\text{Cr}_{0.1}\text{O}_{1.95}\text{S}_{0.05}$	5.397	2.810	5.360	115.584	81.29	0.03
$\text{LiMn}_{0.9}\text{Cr}_{0.1}\text{O}_{1.9}\text{S}_{0.1}$	5.462	2.828	5.416	115.92	83.66	0.11

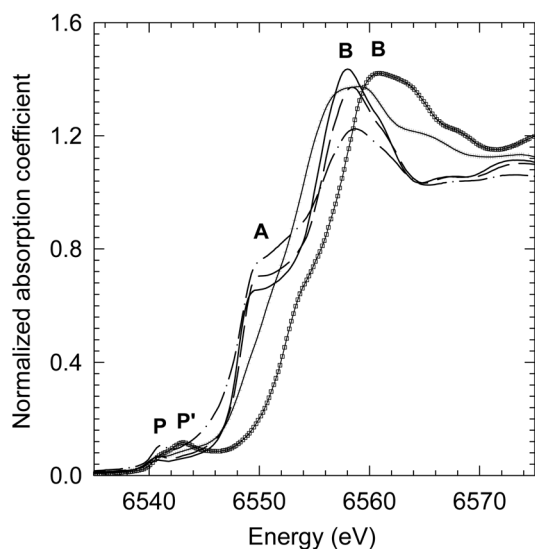


Figure 2. Mn K-edge XANES spectra for the layered $\text{LiMn}_{0.9}\text{Cr}_{0.1}\text{O}_{2-x}\text{S}_x$ compounds with $x = 0$ (solid lines), 0.05 (dashed lines), and 0.1 (dot-dashed lines), in comparison with those for the references Mn_2O_3 (crosses) and MnO_2 (squares).

corresponding to the $1s \rightarrow 3d$ transitions are observed in all the spectra presented here. Even though they are not allowed by the electronic dipolar selection rule, $\Delta l = \pm 1$, the pre-edge peaks become discernible due to the mixing of $4p$ and $3d$ states.¹³ In this context, the negligible intensity of this peak implies that all the manganese ions in the samples under investigation are stabilized in the octahedral site with an inversion center, since this symmetry does not allow the effective hybridization of $4p-3d$ orbitals.¹³ In addition, it has been well-known that the shape and energy of this feature reflect sensitively the oxidation state of manganese ions.¹⁴ That is, two pre-edge peaks P and P' appear for manganese oxide containing considerable amount of tetravalent manganese ions whereas only one feature P at lower energy is observable for trivalent manganese oxide. As can be seen clearly from Figure 2, regardless of sulfur content, all the present $\text{LiMn}_{0.9}\text{Cr}_{0.1}\text{O}_{2-x}\text{S}_x$ compounds show only a peak P at lower energy than the reference MnO_2 . This observation provides strong evidence on little influence of the sulfur substitution on the trivalent oxidation state of manganese ions. In the main-edge region, there are two peaks corresponding to the dipole-allowed transitions from the core $1s$ level to the unoccupied $4p$ level. All the present $\text{LiMn}_{0.9}\text{Cr}_{0.1}\text{O}_{2-x}\text{S}_x$ compounds display an intense peak A corresponding to the $1s \rightarrow 4p$ transition with shakedown process⁴ and the intensity of this peak is enhanced with increasing sulfur content. Since the strong peak A is an indicator of trivalent manganese ion stabilized in the Jahn-Teller (JT) distorted octahedra,⁴ the observed increase of the peak intensity upon the sulfur substitution indicates the enhancement of JT deformation around manganese ion. In addition, another peak B appears commonly for all the present manganese oxides. It has been well-documented that a sharp and intense peak B occurs from the well-ordered network of edge-shared MnO_6 octahedra.¹⁴ In this regard,

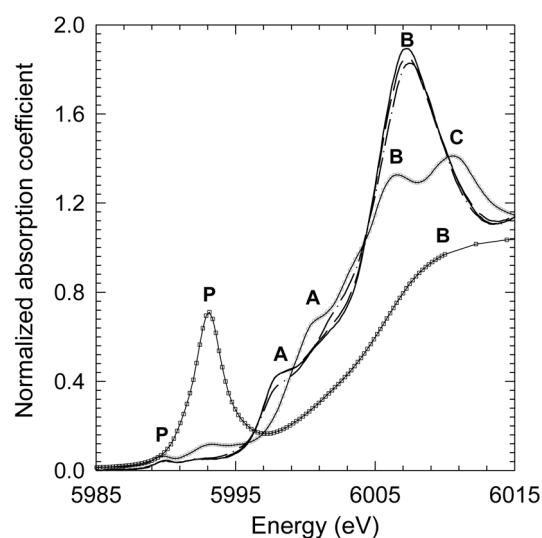


Figure 3. Cr K-edge XANES spectra for the layered $\text{LiMn}_{0.9}\text{Cr}_{0.1}\text{O}_{2-x}\text{S}_x$ compounds with $x = 0$ (solid lines), 0.05 (dashed lines), and 0.1 (dot-dashed lines), in comparison with those for the references Cr_2O_3 (circles) and CrO_3 (squares).

the observed depression and broadening of this peak after the sulfur substitution underscores that the crystal structure of manganese oxide layer becomes more disordered by replacing a fraction of oxide ions with larger sulfide ions.

Figure 3 illustrates the Cr K-edge XANES spectra for $\text{LiMn}_{0.9}\text{Cr}_{0.1}\text{O}_{2-x}\text{S}_x$ ($x = 0, 0.05$, and 0.10), together with the reference spectra for Cr_2O_3 and CrO_3 . The edge energies of layered lithium manganates are almost identical to that of Cr_2O_3 , indicative of the trivalent oxidation state of chromium in these compounds. While the pre-edge peak P related to the dipole-forbidden $1s \rightarrow 3d$ transition is fairly weak in intensity for Cr_2O_3 with trivalent chromium ion in the octahedral site, a very intense feature P is detected for the reference CrO_3 with the tetrahedral Cr^{+VI} ion.¹⁵ Such an inconsistency is attributed to differences not only in the hole concentration of Cr $3d$ orbitals but also in the local symmetry around chromium, i.e., O_h for the former and T_d for the latter. In this regard, the weak intensity of the pre-edge peak P for $\text{LiMn}_{0.9}\text{Cr}_{0.1}\text{O}_{2-x}\text{S}_x$ reveals that all the chromium ions exist in the octahedral sites of transition metal oxide layer, regardless of sulfur substitution. In the main-edge region, the overall spectral features of $\text{LiMn}_{0.9}\text{Cr}_{0.1}\text{O}_{2-x}\text{S}_x$ remain nearly unchanged before and after sulfur substitution, which is surely contrast to the Mn K-edge case. Such a high stability of CrO_6 octahedra is due to its very large OSSE preventing the deformation of local structure.⁶

We have examined the influence of sulfur substitution on the electrochemical performance of layered lithium manganese oxide. Figure 4 presents the variation of the discharge capacities of $\text{LiMn}_{0.9}\text{Cr}_{0.1}\text{O}_{2-x}\text{S}_x$ ($x = 0, 0.05$, and 0.1) measured with the constant current density of 20 mA/g. All of the present electrode materials show similar electrochemical behaviors, in which the discharge capacity decreases initially and then subsequently increases. Even though the recovery of discharge capacity after the initial several cycles

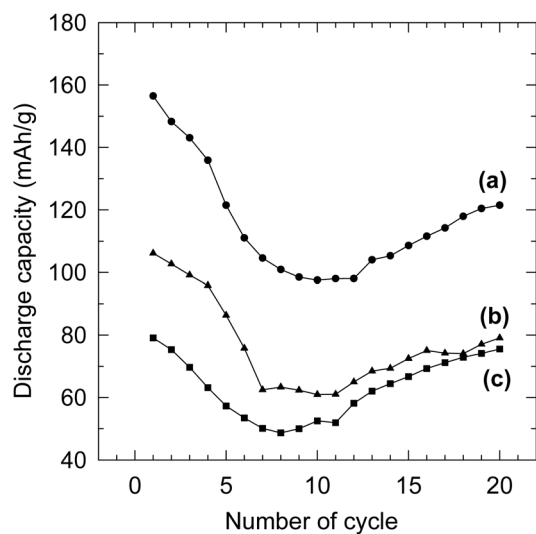


Figure 4. Discharge capacities of the layered $\text{LiMn}_{0.9}\text{Cr}_{0.1}\text{O}_{2-x}\text{S}_x$ compounds with $x =$ (a) 0 (circles), (b) 0.05 (triangles), and (c) 0.1 (squares). The electrochemical measurements were carried out in the potential range of 2.0–4.3 V with the applied current density of 20 mA/g.

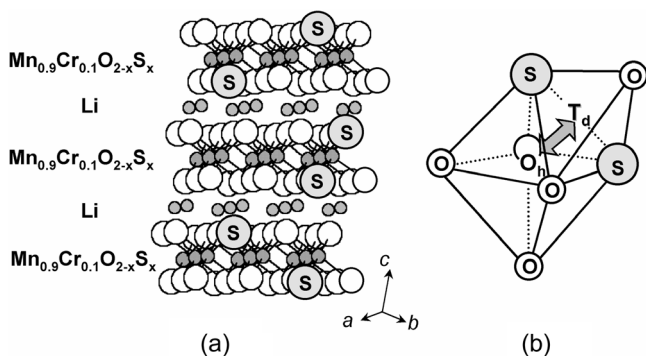


Figure 5. Schematic models for (a) the puckering of the layered lattice of sulfur-substituted lithium manganate and (b) the narrowing of Mn migration path by the incorporation of larger sulfur ions.

is faster for the sulfur-substituted derivative than for the unsubstituted one, the discharge capacity of the former is smaller than that of the latter for entire cycle range applied here, which could be explained by the structural deformation of sulfur-substituted derivatives as follows. As illustrated in Figure 5a, the layered lattice of manganese oxide becomes puckered along the c -axis by replacing oxide ions with larger sulfide ones, leading to the disturbance of effective lithium intercalation/disintercalation through the distortion of Li^+ diffusion path. Moreover, taking into account the fact that substituted sulfur has a lower electronegativity than oxygen,¹⁶ the former can form stronger covalent bonds with interlayer lithium, leading to the depression of Li^+ ion mobility and the subsequent decrease of discharge capacity. Considering the negative side effect of sulfur substitution (*i.e.* the decrease of initial capacity), it would be better to incorporate sulfur ions at low content for the optimization of electrochemical performance of lithium manganese oxide.¹⁰ In the light of

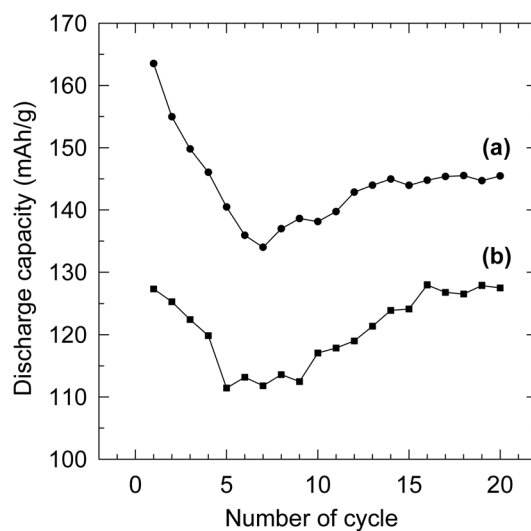


Figure 6. Discharge capacities of the layered $\text{LiMn}_{0.9}\text{Cr}_{0.1}\text{O}_{2-x}\text{S}_x$ compounds with $x =$ (a) 0 (circles) and (b) 0.05 (squares). The electrochemical measurements were carried out in the potential range of 2.0–4.3 V with the applied current density of 6.25 mA/g.

this, we have examined the electrochemical property of lightly substituted $\text{LiMn}_{0.9}\text{Cr}_{0.1}\text{O}_{1.95}\text{S}_{0.05}$ compound with smaller current density of 6.25 mA/g, in comparison with that of the pristine $\text{LiMn}_{0.9}\text{Cr}_{0.1}\text{O}_2$ one. As plotted in Figure 6, the discharge capacity of unsubstituted $\text{LiMn}_{0.9}\text{Cr}_{0.1}\text{O}_2$ is smaller by 11% for the 20th cycle than for the 1st cycle. On the contrary, the sulfur-substituted derivative shows the increase of discharge capacity after the 20th cycle compared to the initial capacity. Moreover, the increasing rate of capacity from a minimum point (*i.e.* the 7th cycle for $\text{LiMn}_{0.9}\text{Cr}_{0.1}\text{O}_2$ and the 5th cycle for $\text{LiMn}_{0.9}\text{Cr}_{0.1}\text{O}_{1.95}\text{S}_{0.05}$) was determined to be 1.29 mAh/g per each cycle for the sulfur-substituted derivative, which is surely faster than that of the pristine material (0.83 mAh/g per each cycle). Moreover, as can be seen clearly from Figure 6, the pristine material unfolds a distinct decrease of slope after the 14th cycle, which is surely different from the sulfur-substituted compound. In this regard, we are able to verify the positive effect of the sulfur substitution on the cyclability of layered lithium manganate, even though we have measured the discharge capacity only for the initial 20th cycles. As mentioned in introduction section, the capacity loss of the layered lithium manganate originates from a structural modification to spinel-type cation ordering caused by the migration of manganese ions into the interlayer lithium sites.⁴ From differential capacity analyses for the present data of $\text{LiMn}_{0.9}\text{Cr}_{0.1}\text{O}_2$ and $\text{LiMn}_{0.9}\text{Cr}_{0.1}\text{O}_{1.95}\text{S}_{0.05}$, it becomes certain that both the compounds do not show the appearance of reduction peaks at 3.95 and 4.1 V during electrochemical cycling. Considering the fact that these peaks are characteristics of spinel lithium manganate phase,¹⁰ both compounds do not experience the distinct structural transition to spinel-type structure. Such excellent stability of both compounds would be due to the improved stability of layered lithium manganate through chromium substitution, as reported previously.⁶ In addition,

we are able to suggest that the replacement of smaller oxide ions with larger sulfide ones makes down the migration paths of Mn ions from octahedral sites to interstitial tetrahedral ones, see Figure 5b.⁴ As a result of the shrinkage of Mn migration path, the stability of layered lithium manganese oxide is expected to be larger for the sulfur-substituted sample than for the unsubstituted one, which would be partially responsible for the enhancement of cyclability after the sulfur substitution. However, it should be mentioned that the JT distortion of MnO₆ octahedra becomes enhanced upon the sulfur substitution, as found from the present Mn K-edge XANES results (Figure 2). Such an increased distortion would relieve the positive effect of sulfur substitution on the shrinkage of Mn migration path. In addition to the prevention of Mn migration, the larger sulfur ions are expected to play a role as a kind of pillars in layered structure, which would promote the disintercalation/intercalation of interlayer lithium ions. This effect would make an additional contribution to the rapid recovery of discharge capacity for the sulfur-substituted derivatives.

Conclusion

In this work, we have synthesized sulfur-substituted LiMn_{0.9}Cr_{0.1}O_{2-x}S_x (0 ≤ x ≤ 0.1) layered oxides via the solid state reaction and characterized the evolutions of chemical bonding nature and electrochemical performance upon sulfur substitution. Powder XRD and EDS analyses revealed that sulfur ions are successfully incorporated into the monoclinic-layered structure of lithium manganese oxide. According to XANES results at Mn and Cr K-edges, the substitution of oxygen with sulfur induces a remarkable structural deformation of MnO₆ octahedra but does not affect significantly the local symmetry around chromium ions. From electrochemical measurements, it was found that the sulfur substitution gives rise to the depression of discharge capacity as well as to the improvement of cyclability. On the basis of the spectroscopic evidences presented here, we are able to explain successfully the variation of electrochemical property upon the sulfur substitution by the increase of structural deformation of manganese oxide layer,

the depression of Mn migration, the formation of covalent Li-S bonds, and the pillaring effect of larger sulfur anion.

Acknowledgement. This work was performed by the financial support of National Nuclear R&D Programs of the Ministry of Science and Technology (MOST), Republic of Korea, and supported partly by the SRC/ERC program of MOST/KOSEF (grant: R11-2005-008-03002-0). The experiments at Pohang Accelerator Laboratory (PAL) were supported in part by MOST and POSTECH. S. H. Lee and S.-J. Hwang thank to the Ministry of Education for the Brain Korea 21 fellowship.

References

1. Nagaura, T.; Tazawa, K. *Prog. Batteries Solar Cells* **1990**, *9*, 20.
2. Thackeray, M. M. *Prog. Solid State Chem.* **1997**, *25*, 1.
3. Armstrong, A. R.; Gitzendanner, R.; Robertson, A. D.; Bruce, P. G. *Nature* **1998**, 1833.
4. Hwang, S.-J.; Park, H. S.; Choy, J.-H.; Campet, G. *Chem. Mater.* **2000**, *12*, 1818.
5. Vitins, G.; West, K. *J. Electrochem. Soc.* **1997**, *144*, 2587.
6. (a) Hwang, S.-J.; Park, H. S.; Choy, J.-H.; Campet, G. *J. Phys. Chem. B* **2000**, *104*, 7612. (b) Armstrong, A. R.; Gitzendanner, R.; Robertson, A. D.; Bruce, P. G. *Chem. Commun.* **1998**, 1833.
7. Park, Y. J.; Hong, Y.-S.; Wu, X.; Kim, M. G.; Ryu, K. S.; Chang, S. H. *Bull. Kor. Chem. Soc.* **2004**, 511.
8. Park, S.-H.; Park, K. S.; Sun, Y. K.; Nahm, K. S. *J. Electrochem. Soc.* **2000**, *147*, 2116.
9. Sun, Y. K.; Park, G.-S.; Lee, Y.-S.; Yoashio, M.; Nahm, K. S. *J. Electrochem. Soc.* **2001**, *148*, A994.
10. Park, S.-H.; Lee, Y.-S.; Sun, Y. K. *Electrochem. Commun.* **2003**, *5*, 124.
11. Teo, B. K. *EXAFS: Basic Principles and Data Analysis*; Springer-Verlag: Berlin, 1986.
12. Shannon, R. D. *Acta Crystallogr. A* **1976**, *32*, 751.
13. Treuil, N.; Labrugère, C.; Menetrier, M.; Portier, J.; Campet, G.; Deshayes, A.; Frison, J. C.; Hwang, S. J.; Song, S. W.; Choy, J. H. *J. Phys. Chem. B* **1999**, *103*, 2100.
14. Hwang, S.-J.; Kwon, C. W.; Portier, J.; Campet, G.; Park, H. S.; Choy, J.-H.; Huong, P. V.; Yoshimura, M.; Kakihana, M. *J. Phys. Chem. B* **2002**, *106*, 4053.
15. Hwang, S.-J.; Choy, J.-H. *J. Phys. Chem. B* **2003**, *107*, 5791.
16. Huheey, J. H.; Keiter, E. A.; Keiter, R. L. *Inorganic Chemistry: Principles of Structure and Reactivity*; HarperCollins: New York, 1993; p 171.